JOURNAL OF GUIDANCE, CONTROL, AND DYNAMICS
Vol. 19, No. 1, January–February 1996

Satellite Pitch Dynamics in the Elliptic Problem of Three Bodies

Joshua Ashenberg*
Technion—Israel Institute of Technology, Haifa 32000, Israel

An extension of the restricted elliptic three-bodies problem to include the gravity gradient is presented. The nonlinear pitch dynamics of a satellite located at an equilibrium point is investigated. A closed-form solution for the circular case is presented. Small perturbations solutions, periodic solutions, and global dynamics via Poincaré maps and bifurcation diagrams are studied. The pitch is most stable and has the largest liberation manifold and the smallest chaotic region at L_2. A numerical example of pitch in the Earth–moon system is presented.

Introduction

IN the restricted problem of three bodies, two bodies of finite mass (the primaries) revolve around each other, while a third body of infinitesimal mass moves in their field.[1] In the idealized and simple problem, the primaries are in a circular orbit. A more complicated but more realistic case is when the primaries are in elliptic orbits. Contrary to the circular case, the elliptic problem is nonintegrable. In the current problem, although the mass of the third body is infinitesimal relative to the primaries, it has a finite dimension. Thus, the system involves additional degrees of freedom due to the third body rotation around its center of mass.

The problem of gravity gradient for the two-body system has been extensively investigated in the past. The classical solutions, usually formulated by small perturbations methods, were extensively studied by Beletskii.[2] The modern approaches utilize the global dynamics analysis for gravity-gradient problems. Wisdom et al.[3] show that irregularity in the satellite shape may cause chaotic tumbling. Periodic solutions and their stability are presented by Modi and Brereton.[4] A comprehensive work by Karasopoulos and Richardson[5] shows bifurcation diagrams that reveal the dependence on eccentricity, especially the transition to chaos with increasing eccentricity. The cited references are restricted to the pitch motion; the nonlinear dynamics of higher dimensional systems is hard to analyze or to visualize. Robinson[6,7] extended the gravity gradient to the restricted problem of three bodies. The results, however, are limited to the case where the primaries are in a circular orbit. Only the linear motion is investigated.

The current paper extends the investigation to the global dynamics in the elliptic case. The results can be applied to the preliminary design of variety of projects. For example, a future lunar space station, communication satellites, or space power station (SPS) at the libration points of Earth–moon, space telescope or SPS at the libration points of Earth–sun. The paper suggests the proper inertia and the initial rotation rates for the desired pitch motion.

Before proceeding further, consider the following comparison. Let $F^{(j)}$ and $G^{(j)}$ be the force and the gravity-gradient torque due to a source with mass m_j and distance r_j. The ratios of the maximal forces and torques due to each source are

$$\frac{G^{(1)}_{\max}}{G^{(2)}_{\max}} = \frac{m_1 \cdot r_2^3}{m_2 \cdot r_1^3}; \qquad \frac{F^{(1)}_{\max}}{F^{(2)}_{\max}} = \frac{m_1 \cdot r_2^2}{m_2 \cdot r_1^2} \tag{1}$$

Table 1 presents these ratios for a satellite located at the equilibrium points (Fig. 1) and for a satellite in a geosynchronous orbit, in the Earth–moon system. The moon as a torque source is dominant at L_1 and at L_2; the Earth is always dominant in terms of force.

Next, the pitch in the elliptic three-body problem will be formulated and analyzed with application to the Earth–moon system.

Received May 11, 1994; revision received Jan. 5, 1995; accepted for publication June 15, 1995.

*Research Fellow, Faculty of Aerospace Engineering; currently Visiting Scientist, Harvard–Smithsonian Center for Astrophysics, Mail Stop 80, Cambridge, MA 02138. Member AIAA.

Model

The current problem is concerned with the planar three-degrees-of-freedom motion (two orbital and one rotation). Referring to Fig. 1, the two primaries m_1 and m_2 are rotating in an elliptic orbit about their mutual center of mass: the origin of coordinates; a and e are the semimajor axis and the eccentricity, respectively. The coordinates x and y are attached to the primaries and rotate with the true anomaly f relative to the fixed coordinates X and Y. The radius vectors of the primaries are $\mu \boldsymbol{r}$ and $(1-\mu)\boldsymbol{r}$ where μ is the mass ratio. The third body m, is located at a distance r_j from each primary m_j. Let $\hat{\boldsymbol{b}}_k$, $k = 1, 2, 3$ be the unit vectors parallel to the rotating coordinates, and let $\hat{\boldsymbol{p}}_k$ be the principal axes of the third body. The orientation of this body is characterized by the rotation α. This pitch angle describes the pendulumlike motion of the third body in the local vertical coordinates. To derive the equations of motion, one formulates the Hamiltonian consisting of the sum of the kinetic energy T and the potential function U, where

$$T = \tfrac{1}{2}m\left[(\dot{x} - f\dot{y})^2 + (\dot{y} + f\dot{x})^2\right] + \tfrac{1}{2}C\,(\dot{\alpha} + \dot{f})^2$$
$$U = Gm\sum_{j=1}^{2}\frac{m_j}{r_j} + \frac{1}{2}G\sum_{j=1}^{2}\frac{m_j}{r_j^3}\left(\mathrm{tr}\boldsymbol{I} - 3I_{r_j}\right) \tag{2}$$

The first terms of T and U are due to the orbital motion and the second due to the rotation, respectively. These terms will be denoted by the subscripts orbit and rot, respectively. C is the orthogonal component of the moment of inertia dyadic $\boldsymbol{I}$ ($A = I_1$, $B = I_2$, $C = I_3$).

Table 1 Forces and torques due to Earth–moon

Location	G_E/G_M	F_E/F_M
Geosynchronous orbit	43,700	5370
L_1	1/4.11	1.68
L_2	1/2.17	2.60
L_3	655	326
L_4	81	81

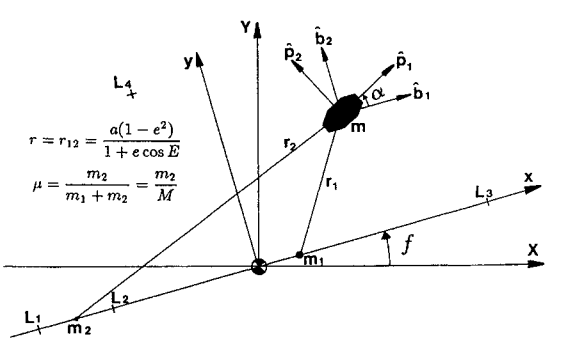

Fig. 1 Model.

U_{rot} is obtained by the MacCullagh formula.[8] It assumes that the typical dimension of the body is very small relative to the radius vector [approximation to the order of $(R_{\text{body}}/r_j)^4$]. I_{r_j} is the projection of the moment of inertia along the radius vector from each primary. In dyadic notations, $I_{r_j} = \hat{r}_j \cdot \boldsymbol{I}_p \cdot \hat{r}_j$, where $\boldsymbol{I}_p = A\,\hat{p}_1\hat{p}_1 + B\,\hat{p}_2\hat{p}_2 + C\,\hat{p}_3\hat{p}_3$. The vector field described by U is, in general, irrotational (but not conservative). It is conservative only in the specific case where r_j is constant, i.e., a circular orbit. Let $\{x, y, \alpha\}$ and $\{p_x, p_y, p_\alpha\}$ denote the coordinates and the momenta, respectively. The corresponding Hamiltonian is

$$H = \left(p_x^2/2m\right) + \left(p_y^2/2m\right) + \left(p_\alpha^2/2C\right) + (yp_x - xp_y + p_\alpha)\dot{f} - (U_{\text{orbit}} + U_{\text{rot}}) \tag{3}$$

This Hamiltonian is a first integral only if $\dot{f} = 0$. In the elliptic case, $\dot{f}$ is not constant so the problem is nonintegrable. Transforming the canonical equations into the configuration space results in the following equations of motion:

$$\begin{aligned} \ddot{x} - 2\dot{f}\dot{y} &= \dot{f}^2 x + \ddot{f}y + \frac{1}{m}\left(\frac{\partial U_{\text{orbit}}}{\partial x} + \frac{\partial U_{\text{rot}}}{\partial x}\right) \\ \ddot{y} + 2\dot{f}\dot{x} &= \dot{f}^2 y - \ddot{f}x + \frac{1}{m}\left(\frac{\partial U_{\text{orbit}}}{\partial y} + \frac{\partial U_{\text{rot}}}{\partial y}\right) \\ \ddot{\alpha} + \frac{3G}{2C}\sum_{j=1}^{2}\frac{m_j}{r_j^3}\frac{\partial I_{r_j}}{\partial \alpha} &= \ddot{f} \end{aligned} \tag{4}$$

Note that the orbital motion and the rotation are coupled. The first two can be written in complex form

$$\ddot{z} + 2i\dot{f}\dot{z} - \dot{f}^2 z = -i\ddot{f}z + (1/m)\nabla_z(U_{\text{orbit}} + U_{\text{rot}}) \tag{5}$$

where $z \overset{\text{def}}{=} x + iy$. Changing the independent variable, $t \to f$, and defining the dimensionless pulsating coordinates $\zeta \overset{\text{def}}{=} z/r$, results in

$$\frac{\mathrm{d}^2\zeta}{\mathrm{d}f^2} + 2i\frac{\mathrm{d}\zeta}{\mathrm{d}f} = \frac{1}{1 + e\cos f}\left[\zeta + \frac{r^2}{GMm}\nabla_z(U_{\text{orbit}} + U_{\text{rot}})\right] \tag{6}$$

U_{rot} depends on the irregularity of the shape $(B - A)$ and the attitude orientation α. Comparing orders of magnitude, $U_{\text{rot}}/U_{\text{orbit}} = \mathcal{O}(R/r)^2$, where R is a typical dimension of the body m. Thus, U_{rot} can be treated as a very small perturbation in the orbital motion. More specifically, with the third body located at one of the equilibrium points in the pulsating coordinates $(L_1, \ldots, L_5)$, U_{rot} is considered as a small perturbation about the equilibrium. L_1, L_2, and L_3 are along the radius vector $\boldsymbol{r}_{12}$, whereas L_4 and L_5 are the triangular points. L_5 is a mirror image of L_4 with respect to $\boldsymbol{r}_{12}$.

The rest of this work is dedicated to the problem of the pitch. Neglecting U_{rot}, the problem degenerates now to a rotational motion of a satellite located at a pulsating equilibrium point.

Pitch Equation

The pitch dynamics in the two-body gravity-gradient problem depend on the body shape and on the orbit semimajor axis and eccentricity. In the three-body case, the particular equilibrium point plays a major role. Substituting the particular values for each equilibrium point, the equation for the pitch has the following form: At L_1, L_2, and L_3

$$\ddot{\alpha} + \tfrac{3}{2}(GM/r^3)\left[(1-\mu)/\rho_1^3 + \left(\mu/\rho_2^3\right)\right]K_2 \sin 2\alpha = -\ddot{f} \tag{7a}$$

whereas at L_4 (and L_5)

$$\ddot{\alpha} + (3GM/4r^3)[\sqrt{3}(1-2\mu)\cos 2\alpha - \sin 2\alpha]K_2 = -\ddot{f} \tag{7b}$$

Here $K_2 \overset{\text{def}}{=} (B - A)/C$ and $\rho_j \overset{\text{def}}{=} r_j/r$. The equation, with the true anomaly as the independent variable, is more convenient for further applications. A straightforward transformation leads to

$$(1 + e\cos f)\alpha'' - 2e\sin f(1 + \alpha') + \tfrac{3}{2}\left[(1-\mu)/\rho_1^3 + \mu/\rho_2^3\right]K_2 \sin 2\alpha = 0 \tag{8a}$$

for L_1, L_2, and at L_3, and

$$(1 + e\cos f)\alpha'' - 2e\sin f(1 + \alpha') + \tfrac{3}{4}[\sqrt{3}(1-2\mu)\cos 2\alpha - \sin 2\alpha]K_2 = 0 \tag{8b}$$

for L_4, where the prime denotes derivative with respect to the true anomaly. As in the two-body elliptic case, the pitch equation has time-dependent coefficients as well as an oscillatory forcing term. In the particular case of a circular orbit, the equation is time independent and has a first integral. The local dynamics will be formulated next.

With $\bar{\alpha}$ defined as the pitch angle at equilibrium in a circular orbit, it equals zero at the collinear points (L_1, L_2, L_3). In other words, one of the principal axes must be aligned with the radius vector of both primaries. At the Lagrangian points (L_4, L_5), on the other hand, the equilibrium depends on the function $g = \sqrt{3}(1-2\mu)\cos 2\alpha - \sin 2\alpha$. It can be written as

$$g = -\sqrt{1 + 3(1-2\mu)^2}\,\sin(2\alpha - 2\bar{\alpha})$$

where $\bar{\alpha} = \frac{1}{2}\arctan[\sqrt{3}(1-2\mu)]$. The pitch equation at L_4 now can be rewritten in the form

$$(1 + e\cos f)\tilde{\alpha}'' - 2e\sin f(\tilde{\alpha}' + 1) - \tfrac{3}{4}\sqrt{1 + 3(1-2\mu)^2}K_2 \sin 2\tilde{\alpha} = 0 \tag{9}$$

where $\tilde{\alpha} = \alpha - \bar{\alpha}$. It is important to emphasize at this point that the pitch equilibrium is limited to the circular problem of three bodies. These equilibrium attitudes, in the elliptic problem, will be considered as reference attitudes, perturbed by the ellipticity. Inspecting the last form of the pitch equation indicates that the pitch equations for the two body and for the three body are analogous. It will be recalled that the two-body pitch equation is as follows[2]:

$$(1 + e\cos f)\alpha'' - 2e\sin f(\alpha' + 1) + \tfrac{3}{2}K_2 \sin 2\alpha = 0 \tag{10}$$

Thanks to this analogy, it is sufficient to solve the two-body pitch with a suitable value for the inertia coefficient K_2. Let us define an equivalent inertia coefficient, K_{eq} and a function F,

$$F \overset{\text{def}}{=} \begin{cases} 1; & \text{for the two body} \\ (1-\mu)/\rho_1^3 + \mu/\rho_2^3; & \text{for } L_1, L_2, L_3 \\ -\frac{1}{2}\sqrt{1 + 3(1-2\mu)^2}; & \text{for } L_4 \end{cases} \tag{11}$$

The equivalent inertia coefficient $K_{\text{eq}} = F \cdot K_2$ replaces K_2 in the two-body equation. Note that $K_{\text{eq}} = F$ for the case of a dumbbell satellite. F is a function of the primaries' mass ratio (Fig. 2). It is maximal at L_2 for $\mu = \frac{1}{2}$, and F is minimal at L_4 and is actually very close to the value $F = 1$, the two-body case. In the practical applications μ is very small; hence, $F(L_1) \approx 3 \to 4$, $F(L_2) \approx 4 \to 6$, $F(L_3) \approx 1^+$, and $F(L_4) \approx 1^-$. An efficient approximation for F is described in Appendix A. The large values of F at L_1 and L_2

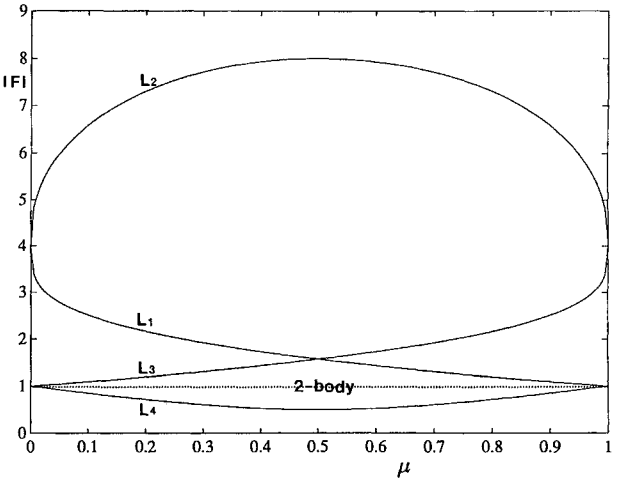

Fig. 2 Function F.

are unique to the three-body problem. Since $K_2 \leq 1$ due to physical constraints, all of the previous analyses of gravity-gradient satellites were limited to this domain. Because of the significantly larger restoring torque at L_1 and L_2, the domain must be extended to $K_{eq} > 1$. These results are compatible with physical intuition as shown subsequently. Let us consider the circular case. At L_1, L_2, and L_3, the function $F > 0$; therefore, the satellite is stable in pitch if $K_2 > 0$, i.e., $B > A$. In other words, the minor principal axis is aligned with the primaries radius vectors, as in the two-body problem. At L_4, the function $F < 0$, and the stability condition requires $K_2 < 0$, i.e., $A > B$. Let us, for example, visualize the case $\mu = \frac{1}{2}$ ($m_1 = m_2$). The equilibrium pitch angle $\bar{\alpha}$ is zero, and so the minor principal axis points toward the primaries mass center. In reality $\mu \ll \frac{1}{2}$; therefore, $\bar{\alpha} > 0$ and the minor principal axis is tilted toward the largest primary. The stable configurations are demonstrated in Fig. 3.

Integrable Case

The particular case of a circular orbit is worth consideration for the following reasons. First, the problem is solvable. Second, most of the typical orbits in the solar system are nearly circular, hence, the circular solution may be attempted first. Defining the function W as $W(\mu, L_j, K_2) \stackrel{\text{def}}{=} 3K_{eq}$, the first integral of the pitch equation is

$$\alpha'^2 + W(\mu, L_j, K_2)\sin^2\alpha = 2h \tag{12}$$

The topology of the phase space is determined by the modulus k, $k^2 = 2h/W$. It is a function of the orbital characteristics, the moment of inertia, as well as the initial conditions. The liberation manifold $k < 1$ is wrapped by the separatrices $k = 1$. This manifold, as a function of the primaries mass ratio, is plotted in Fig. 4. It is the widest at L_2 and the narrowest at L_4. The closed-form solution for the pitch is analogous to the following nonlinear pendulum solution:

$$\sin\alpha = k \cdot sn\{\sqrt{W}(f - f_0) + F_0; k\} \tag{13}$$

Here, sn is the Jacobi elliptic sine function, F_0 is the elliptic integral of the first kind with argument ϕ_0, where $\sin\alpha = k\sin\phi$. F_0 depends solely on the initial conditions. Let m and n be the number of pitch librations and the number of the orbits, respectively. The periodic solutions satisfy the condition

$$K_2 = \frac{4}{3\pi^2}\frac{1}{|F(\mu, L_j)|}K_{(k)}^2\left(\frac{m}{n}\right)^2 \tag{14}$$

where K is the Legendre's complete integral of the first kind. Figure 5 presents a map for various periodic solutions (m, n) in libration ($k < 1$) or tumbling ($k > 1$). The literature is confined to $K_{eq} \leq 1$. The current research reveals higher m/n ratios, especially for L_2, as can be seen from Fig. 6. The existence of the high frequencies is obvious from observing the case of a small amplitude, $k \to 0$. In that case $m/n = \sqrt{(3K_{eq})}$, therefore, the bound for the frequency spectrum is $m/n < \sqrt{24}$. In general, the periodic

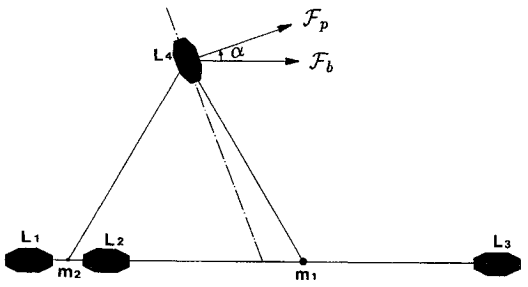

Fig. 3 Stable configuration.

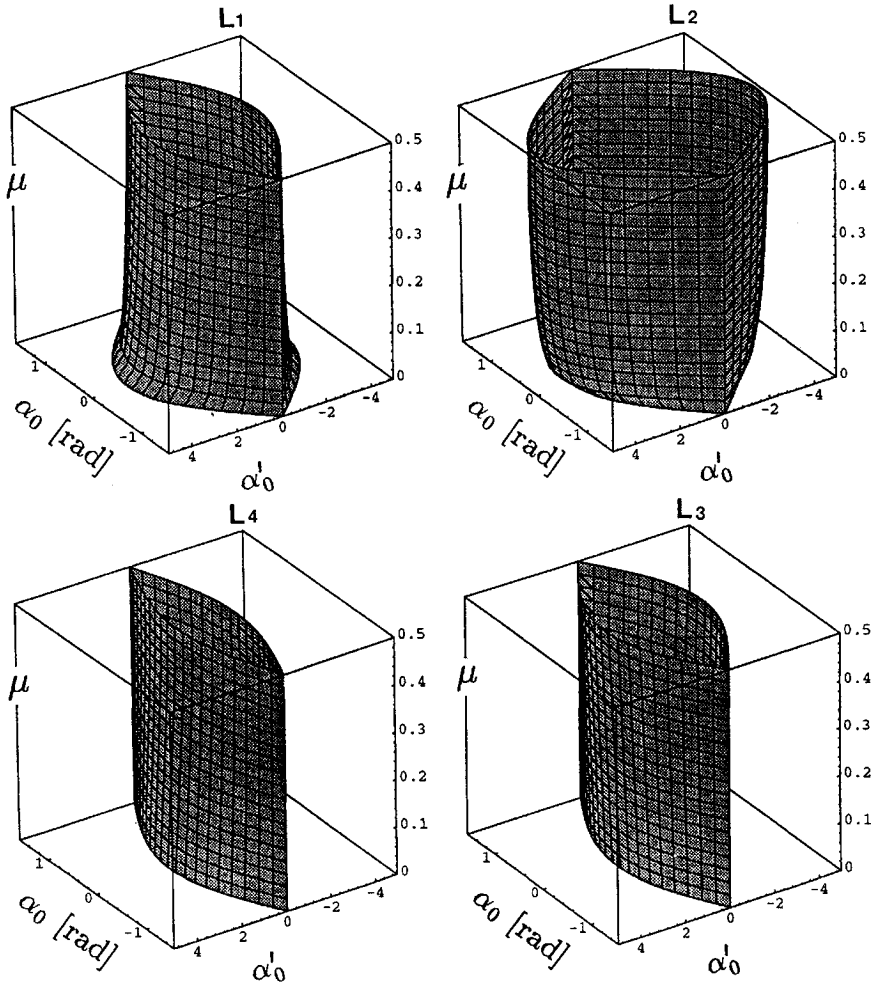

Fig. 4 Libration manifold.

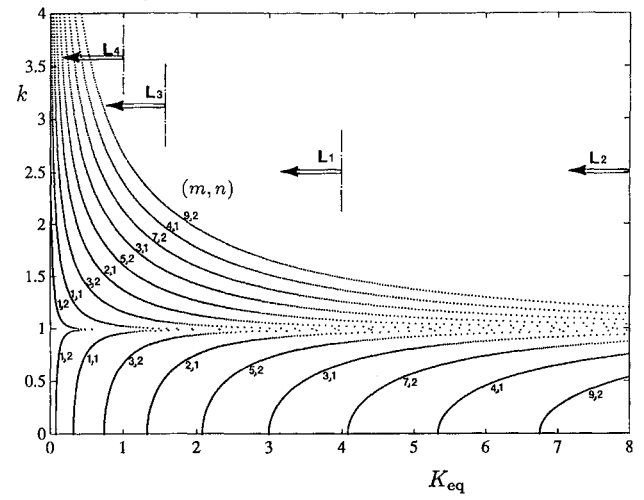

Fig. 5 Conditions for periodic solutions in circular orbits.

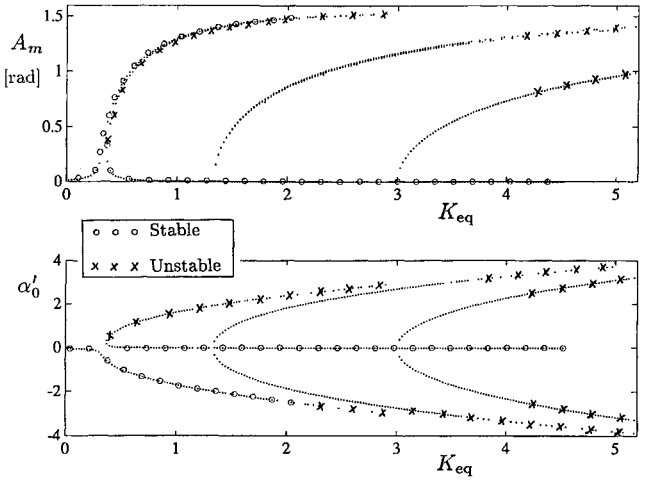

Fig. 6 Amplitude of periodic solutions, $e = 0.01$.

solutions are obtained recursively. For small amplitude, however, an approximate explicit solution can be formulated as presented in Appendix B. Applying the results from Appendix B, the libration manifold of initial conditions (α_0, α_0') is formulated explicitly by the following approximation:

$$\sin^2\alpha_0 + \alpha_0'^2/W = 4[\sqrt{W}(n/m) - 1] - 9[\sqrt{W}(n/m) - 1]^2 + \tfrac{31}{2}[\sqrt{W}(n/m) - 1]^3 + \cdots \quad (15)$$

Nonintegrable Case

The equation of motion for the elliptic case in nonsolvable, in general, for the following three reasons: nonlinearity, periodic coefficients, and a forcing term. Approximate solutions can be obtained for small amplitudes and are restricted to small eccentricities. Various techniques for the two-body case are presented by Beletskii.[2] For large amplitude, numerical techniques must be applied. The global dynamics might be very rich as expressed in the simple, but unsolvable, problem of forced pendulum.[9] The order of the pitch dynamical system in the elliptic case is three, one higher than in the corresponding circular case. Hence, in addition to the periodic and quasiperiodic solutions, chaotic solutions are possible as well.

Linear Solution

Starting with the small-amplitude solution, the linearized pitch equation for small $\delta\alpha$ is

$$(1 + e\cos f)\delta\alpha'' - 2e\sin f\,\delta\alpha' + W\delta\alpha = 2e\sin f \quad (16)$$

The linear equation can be converted into the Hill's type of equation by the transformation[10] $\beta = (1 + e\cos f)\cdot\delta\alpha$. The resulting Hill's equation is

$$\beta'' + \Omega_{(f)}^2\beta = 2e\sin f; \qquad \Omega^2 \stackrel{\text{def}}{=} \frac{e\cos f + W}{1 + e\cos f} \quad (17)$$

Notice that in the two-body case[11] $W = 3K_2$. The eccentricity-forcing solution is of interest. A formal expansion of β and Ω^2 in small eccentricity, such that

$$\beta = \beta_0 + e\beta_1 + e^2\beta_2 + \cdots$$
$$\Omega^2 = W + \sum_{k=1}^{\infty}(-1)^{k-1}e^k(1 - W)\cos^k f \quad (18)$$

leads to the following forced response:

$$\delta\alpha = -\frac{2e}{1 - W}\sin f + \frac{3e^2}{(1 - W)(4 - W)}\sin 2f - \frac{12e^3}{(1 - W)(4 - W)(9 - W)}\sin 3f + \cdots \quad (19)$$

The solution indicates the parametric values for resonance: $W = 1, 4, 9, \ldots$. Here is an essential characteristic of the current problem. In the two-body case, only a single resonance occurs: $W = 1 (K_2 = \frac{1}{3})$. The other singularities do not contribute resonance because $K_2 \leq 1$. In the present problem $W \leq 24$ and, therefore, higher resonance numbers are possible, depending on L_j and μ. The W sets for resonance are $\{1, 4, 9\}$, $\{1, 4, 9, 16\}$, $\{1, 4\}$, and $\{1\}$ for $L_1, \ldots, L_4$. Note that the amplitude of each resonance number k is on the order of e^k. Therefore, $W = 1$ gives rise to the primary resonance whereas the higher numbers result in a more restrictive amplitude (in the linear case). Further information can be obtained by applying the Krylov–Bogoliubov–Mitropolsky (KBM) method.[12] Writing the linear approximation as

$$\beta'' + W\beta = \left(\sum_{k=1}^{\infty}(-1)^k e^k(1 - W)\cos^k f\right)\cdot\beta + 2e\sin f \quad (20)$$

a solution is sought in the form

$$\beta = a\cos\psi + eu_1(a, \psi, f) + e^2u_2(a, \psi, f) + \cdots \quad (21)$$

where the amplitude a and the phase ψ satisfy the differential equations

$$a' = eA_1(a) + e^2A_2(a) + \cdots$$
$$\psi' = \sqrt{W} + eB_1(a) + e^2B_2(a) + \cdots \quad (22)$$

Substituting equating coefficients of identical harmonics and removing secular terms results in an approximate solution. The derivation is rather lengthy and will not be presented here. The solution reveals, in addition to the eccentricity resonance, the values of W that cause a parametric resonance (due to the periodicity of the coefficients): $W = \{\frac{1}{4}, \frac{9}{4}, \frac{25}{4}, \frac{49}{4}, \frac{81}{4}\}$. At L_3 and L_4 only the first two are possible. There is another, very simple, way[13] to find the parametric resonance. This requires computing the period advance mapping of the homogeneous equation and then finding the conditions for the periodic solution. Of course, the results are identical with the KBM results.

Small Perturbations and Periodic Solutions

The periodic solutions are of special importance; these are predictable, possibly easy to control, and play an essential role in the global dynamics. So far, periodic solutions for the linear approximation have been considered. Extending Beletskii's[2] method to the three-body case, the nonlinear small amplitude periodic solutions can be found. Because of the addition resonance numbers, a periodic solution in the following form will be sought:

$$\alpha = a_1\sin f + a_2\sin 2f + a_3\sin 3f \quad (23)$$

Substituting, expanding $\sin(a_k \sin kf)$ and $\cos(a_k \sin kf)$ in terms of Bessel functions,[14] and equating coefficients of equal harmonics lead to the following approximate relations:

$$W \cdot J_1(2a_1) - a_1 - 2e = 0$$

$$[W \cdot J_0(2a_1) - 4]a_2 - \tfrac{3}{2}ea_1 = 0 \tag{24}$$

$$[W \cdot J_0(2a_1) - 9]a_3 - 4ea_2 = 0$$

The two branches of a_1 are found from the first implicit relation,[2] whereas the other two give the following amplitudes:

$$a_2 = \frac{\frac{3}{2}ea_1}{W \cdot J_0(2a_1) - 4}$$

$$a_3 = \frac{6e^2 a_1}{[W \cdot J_0(2a_1) - 4][W \cdot J_0(2a_1) - 9]} \tag{25}$$

Since a_1 itself is of order $\mathcal{O}(e)$, the other amplitudes are of order $\mathcal{O}(e^2)$ and $\mathcal{O}(e^3)$, respectively, i.e., the first harmonic is dominant when eccentricity is small. Figure 6 presents an exact (numerical) solution for the amplitude related to the fundamental harmonic ($m = 1, n = 1$). The lower part shows the corresponding initial rates ($\alpha_{(f=0)} = 0$). The stability of the periodic solution is found by formulating the variational equations near the periodic solution α_p

$$(1 + e\cos f)\delta\alpha'' - 2e\sin f\,\delta\alpha' + W\cos 2\alpha_p \delta\alpha = 0 \tag{26}$$

This equation is converted into Hill's equation

$$\delta\beta'' + \left(\frac{W \cdot \cos 2\alpha_p + e\cos f}{1 + e\cos f}\right) \cdot \delta\beta = 0 \tag{27}$$

and then Floquet theory[11] is applied. The approach is to formulate the transition matrix Φ, to find the period of the equation coefficients, and then to compute the period advanced mapping. The mapping is stable if and only if $|\mathrm{tr}\,\Phi| < 2$. Referring to the lower part of Fig. 6, the small amplitude branch and most of the lower branch starting at resonance 1 are stable. The upper branch from resonance 1 is unstable. The other branches are almost stable, whereas, $\mathrm{tr}\,\Phi = 2$ at the branching points.

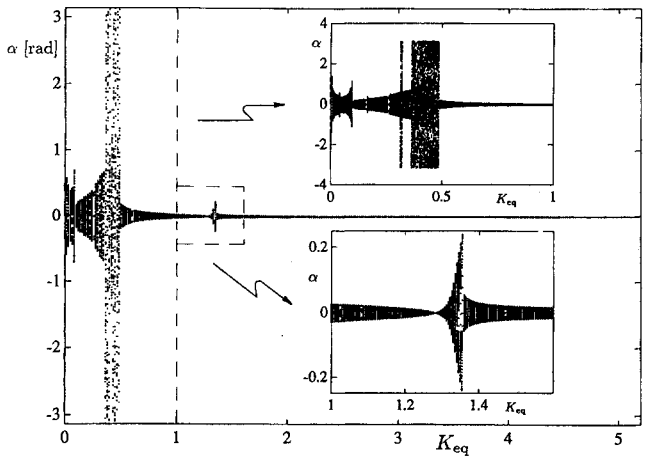

Fig. 7 Pitch angle bifurcation diagram, $e = 0.0549$.

Bifurcation Diagram

For the purpose of exploring the global dynamics, bifurcation diagrams and Poincaré maps are plotted. The bifurcation diagram maps a single initial condition; the zero state was chosen, since it represents a satellite initially at a stable attitude. The possible bifurcation parameters are the eccentricity and the parametric function $W_j(K_2, \mu)$; $j = 1, 2, 3, 4$. As already shown, a reduction can be made by defining K_{eq}. Hence, the parameters are now e and K_{eq}. Bifurcation plots for the eccentricity are of great interest in the two-body case.[5] A transition to chaos appears as e increases. This kind of bifurcation is not presented here because the interesting phenomenon of transition to chaos appears at much higher eccentricities than the typical three-body eccentricities. Figure 7 shows the bifurcation diagram of the pitch angle as a function of the bifurcation parameter K_{eq}, for $e = 0.0549$. As expected, a chaotic zone appears after the first resonance passage ($K_{eq} = \frac{1}{3}$), and it is compatible with the chaos diagram in Ref. 5. The second ($K_{eq} = \frac{4}{3}$) and the third ($K_{eq} = 3$, hard to visualize from the figure) resonances are characterized by abrupt changes. Figure 8 (a magnification of Fig. 7) reveals

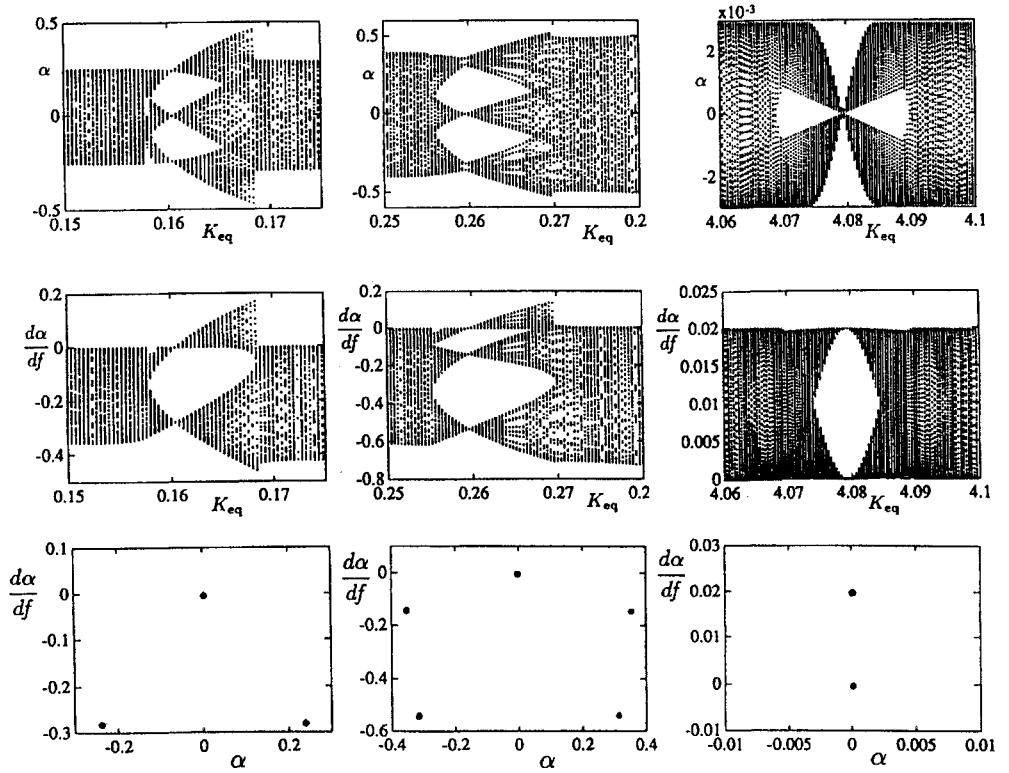

Fig. 8 Bifurcation diagram; magnification and Poincaré maps of periodic solutions.

some periodic orbits. The bifurcation of the pitch angle and the angular rate for these orbits are shown, and the corresponding Poincaré maps are plotted. A fixed point of period 1 was found at $K_{eq} \approx 1.2828$, just before the second resonance. The fixed points at $K_{eq} \approx 0.1604$, 0.2596, and 4.0794 have periods 3, 5, and 2, respectively.

Example: Pitch in the Earth–Moon System

In addition to the practical importance of the Earth–moon system, its eccentricity is representative compared with other planetary systems in the sense that the values of the function F are almost identical. Figure 9 refers to a hypothetical circular Earth–moon system. Only the periods $m \geq n$ are presented. All other periods ($m < n$) can be achieved but are of lesser interest because of their impractical long periods. L_2 has the highest number of periods, up to (7, 2), whereas L_3 and L_4 reach only period (3, 2). Figures 10 and 11 show the Poincaré maps for the extreme cases, L_2 and L_4. A dumbbell satellite was chosen ($K_2 = 1$). The plots are concise and reveal only the essential information. The size of the libration manifold at L_2 is about three times bigger than the corresponding value at L_4. The practical meaning is that a satellite at L_2 (or at L_1) can sustain larger disturbances without tumbling compared with a satellite at L_4 (or at L_3). Both have chaos near the separatrices; the chaotic zone at L_4 is somewhat larger. The family of periodic orbits starting at $\alpha_0 = 0$ was detected. There may be much more periodic solutions, but this family is the most interesting from the practical point of view. Referring to the fixed points, the subscript indicates the period number (2 or 3), whereas the superscript marks the orbit. For example, P_3' consists of three fixed points that belong to the same rotational orbit and has period 3 ($m = 1, n = 3$). The c indicates the center. In addition, a couple and a triple of stable periodic solutions were discovered at L_4. The other periodic orbits are marginally stable or unstable. The marginally stable solutions can be considered as practically stable;

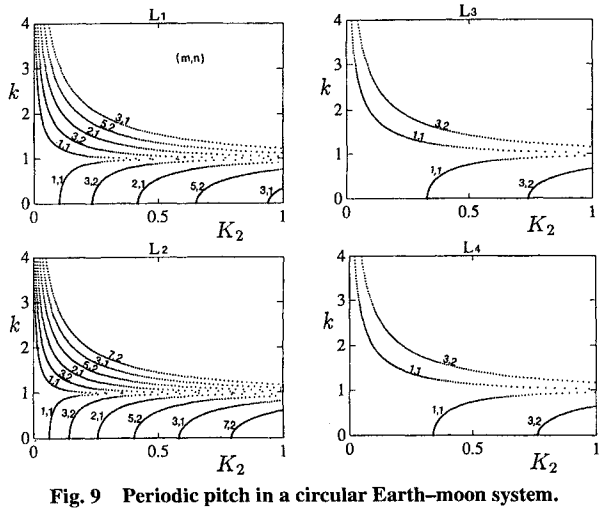

Fig. 9 Periodic pitch in a circular Earth–moon system.

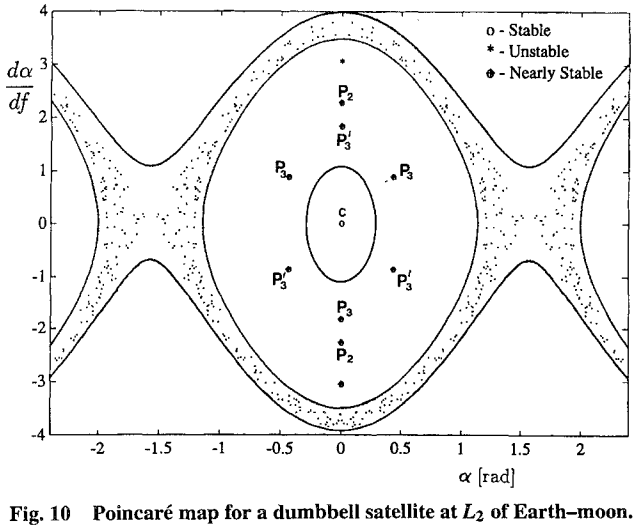

Fig. 10 Poincaré map for a dumbbell satellite at L_2 of Earth–moon.

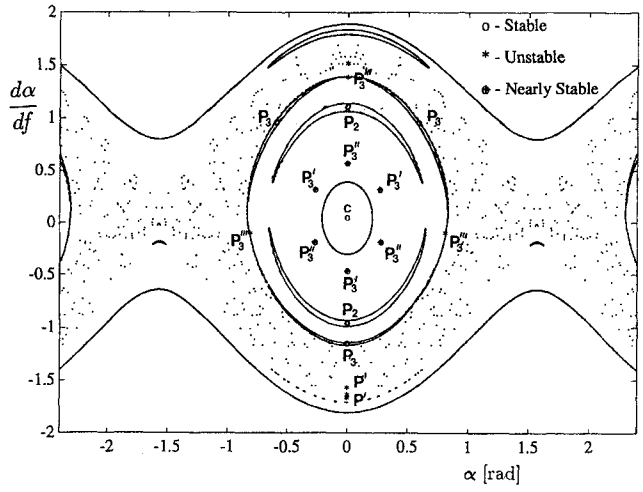

Fig. 11 Poincaré map for a dumbbell satellite at L_4 of Earth–moon.

their characteristic multipliers are nearly one, and so the solution is bounded over the first few orbits.

Concluding Remarks

The pitch equation of motion in the elliptic problem of the three-body case is of the same form as the corresponding equation for the two-body case. The similarity is formulated by defining an equivalent inertia coefficient that may be greater than one leading to a broader spectrum of resonances and periodic solutions. For stable pitch equilibrium attitudes at a collinear point, the minor principal axis is aligned with the primaries radius vectors. At a Lagrangian point the minor principal axis is tilted toward the larger primary. The parameters that play a role are the primaries' mass ratio and the satellite location, in addition to the eccentricity and the inertia (the two-body bifurcation parameters). Various parametric maps demonstrate the influence of these parameters on the pitch dynamics. Generally, L_2 is locally and globally the most stable. L_4 is the least stable. Some further work is needed, for example, computing a chaos map for $K_{eq} > 1$. Generalizing the problem to three-dimensional rotation and examining the robustness of the pitch stability due to small yaw and roll may be of importance.

Appendix A: Approximate Function F

The pitch restoring torque is determined by the function F. It depends on μ and L_j. The location of L_j was computed by the method suggested in Ref. 1. The radius vector for each equilibrium is an iterated solution of a nonlinear algebraic equation, where the initial conditions are written as series expansions in μ. These series are utilized for the approximate solution of $F(\mu, L_j)$. The resulting approximations are the following:

$$F_{(L_1)} = 4 - 2\cdot 3^{\frac{2}{3}}\cdot\mu^{\frac{1}{3}}\left[1 + \frac{4}{4^{\frac{4}{3}}}\mu^{\frac{2}{3}} - \frac{25}{3^{\frac{8}{3}}}\mu + \frac{259}{3^{\frac{15}{3}}}\mu^{\frac{4}{3}} - \frac{1171}{2\cdot 3^{\frac{19}{3}}}\mu^{\frac{5}{3}} + \frac{2800}{3^{\frac{26}{3}}}\mu^2 + \frac{16016}{3^{10}}\mu^{\frac{7}{3}} - \frac{84800}{3^{\frac{34}{3}}}\mu^{\frac{8}{3}} + \frac{5984317}{2\cdot 3^{\frac{44}{3}}}\mu^3\right] + \mathcal{O}\left(\mu^{\frac{10}{3}}\right)$$

$$F_{(L_2)} = 4 + 2\cdot 3^{\frac{2}{3}}\cdot\mu^{\frac{1}{3}}\left[1 + \frac{4}{3^{\frac{4}{3}}}\mu^{\frac{1}{3}} - \frac{2}{3^{\frac{8}{3}}}\mu^{\frac{2}{3}} - \frac{119}{3^{\frac{14}{3}}}\mu - \frac{827}{2\cdot 3^{\frac{19}{3}}}\mu^{\frac{4}{3}} - \frac{1520}{3^{\frac{26}{3}}}\mu^{\frac{5}{3}} - \frac{10697}{3^{10}}\mu^2 - \frac{28046}{3^{\frac{34}{3}}}\mu^{\frac{7}{3}} + \frac{34469}{2\cdot 3^{\frac{44}{3}}}\mu^{\frac{8}{3}}\right] + \mathcal{O}\left(\mu^{\frac{10}{3}}\right) \tag{A1}$$

$$F_{(L_3)} = 1 + (7/8)\mu + (77/192)\mu^2 + (49/288)\mu^3 + \mathcal{O}(\mu^4)$$

$F(L_4)$ is a simple function of μ, and so it is not approximated. The approximations are very satisfactory for $\mu < 0.1$. Moreover, for very small μ, as in the Earth–moon system, even an approximation of order μ is quite satisfactory (error less than 1%).

Appendix B: Periodic Solutions in the Circular Case

The purpose here is to find an explicit formulation for k from the libration periodicity condition

$$m/n = \sqrt{W}/[K(k)] \tag{B1}$$

First, the complete elliptic integral of the first kind is expanded in small k

$$K(k) = \frac{\pi}{2}\left[1 + \sum_{n=1}^{\infty}\left(\frac{\prod_{m=1}^{n}(2m-1)}{\prod_{m=1}^{n}2m}\right)^2 k^{2n}\right] \tag{B2}$$

The periodicity conditions can be written in the form of the following near-identical transformation:

$$z = y + \left(\tfrac{3}{4}\right)^2 y^2 + [(3\cdot 5)/(4\cdot 6)]^2 y^3 + \cdots \tag{B3}$$

where $y \overset{\text{def}}{=} k^2$ and $z \overset{\text{def}}{=} 4\cdot[\sqrt{W}(n/m) - 1]$. The convergency condition requires both to be smaller than one. Inverting the series[14] and expanding the square root results in

$$k = \sqrt{z} - (9/32)z^{\frac{3}{2}} + (167/2048)z^{\frac{5}{2}} + \cdots \tag{B4}$$

This approximation is in a very good agreement with the exact solution for $k < 0.5$.

References

[1]Szebehely, V., *Theory of Orbits*, Academic, New York, 1967, pp. 587–599.

[2]Beletskii, V. V., "Motion of an Artificial Satellite about its Center of Mass," NASA TT F-429, 1966 (translated from Russian).

[3]Wisdom, J., Peale, S. J., and Mignard, F., "The Chaotic Rotation of Hyperion," *Icarus, International Journal of the Solar System*, Vol. 58, May 1984, pp. 137–152.

[4]Modi, V. J., and Brereton, R. C., "Periodic Solutions Associated with the Gravity-Gradient-Oriented System, Parts I and II," *AIAA Journal*, Vol. 7, Nos. 7, 8, 1969, pp. 1217–1225 and pp. 1465–1468.

[5]Karasopoulos, H., and Richardson, D. L., "Chaos in the Pitch Equation of Motion for the Gravity-Gradient Satellite," AIAA Paper 92-4369, Aug. 1992.

[6]Robinson, W. J., "The Restricted Problem of Three Bodies with Rigid Dumb-Bell Satellite," *Celestial Mechanics*, Vol. 8, 1973, pp. 323–331.

[7]Robinson, W. J., "Attitude Stability of a Rigid Body Placed at an Equilibrium Point in the Restricted Problem of Three Bodies," *Celestial Mechanics*, Vol. 10, 1974, pp. 17–33.

[8]Danby, J. M. A., *Fundamentals of Celestial Mechanics*, Willmann–Bell, Richmond, VA, 1988, p. 101.

[9]Baker, G. L., and Gollub, J. P., *Chaotic Dynamics*, Cambridge Univ. Press, New York, 1990, pp. 102–107.

[10]Hayashi, C., *Nonlinear Oscillations in Physical Systems*, Princeton Univ. Press, Princeton, NJ, 1985, p. 85.

[11]Hughes, P. C., *Spacecraft Attitude Dynamics*, Wiley, New York, 1986, pp. 307, 499.

[12]Atlee Jackson, E., *Perspectives of Nonlinear Dynamics*, Cambridge Univ. Press, Cambridge, England, UK, 1981, pp. 264–271.

[13]Arnold, V. I., *Ordinary Differential Equations*, MIT Press, Cambridge, MA, 1990, p. 203.

[14]Abramovitz, M., and Stegun, I. A., *Handbook of Mathematical Functions*, Dover, New York, 1972, pp. 16, 361.